



An Observation Density Based Method for Independent Baseline Searching in GNSS Network Solution

Tong Liu ¹, Yujun Du ^{2,*}, Wenfeng Nie ^{3,4} , Jian Liu ¹, Yongchao Ma ¹ and Guochang Xu ^{1,5}

¹ Laboratory of Navigation and Remote Sensing, Institute of Space Science and Applied Technology (ISSAT), Harbin Institute of Technology, Shenzhen 518055, China

² The Industrial Sciences Group, Sydney, NSW 2060, Australia

³ Institute of Space Sciences, Shandong University, Weihai 264209, China

⁴ State Key Laboratory of Geo-Information Engineering, Xi'an 710000, China

⁵ Key Laboratory of Urban Land Resources Monitoring and Simulation, Ministry of Natural Resources, Shenzhen 518000, China

* Correspondence: eugene@industrialsciences.com.au; Tel.: +61-411-644-071

Abstract: With applications such as precise geodetic product generation and reference frame maintenance, the global GNSS network solution is a fundamental problem that has constantly been a focus of concern. Independent baseline search is a prerequisite step of the double-differenced (DD) GNSS network. In this process, only empirical methods are usually used, i.e., the observation-max (OBS-MAX), which allows for obtaining more redundant DD observations, and the shortest-path (SHORTEST), which helps to better eliminate tropospheric and ionospheric errors between stations. Given the possible limitations that neither of the methods can always guarantee baselines of the highest accuracy to be selected, a strategy based on the ‘density’ of common satellites (OBS-DEN) is proposed. It takes the number of co-viewing satellites per unit distance between stations as the criterion. This method ensures that the independent baseline network has both sufficient observations and short baselines. With single-day solutions and annual statistics computed with parallel processing, the method demonstrates that it has the ability to obtain comparable or even higher positioning accuracy than the conventional methods. With a clearer meaning, OBS-DEN can be an option alongside the previous methods in the independent baseline search.

Keywords: GNSS; independent baseline; GNSS network solution; observation-max; shortest; observation density; minimum spanning tree



Citation: Liu, T.; Du, Y.; Nie, W.; Liu, J.; Ma, Y.; Xu, G. An Observation Density Based Method for Independent Baseline Searching in GNSS Network Solution. *Remote Sens.* **2022**, *14*, 4717. <https://doi.org/10.3390/rs14194717>

Academic Editors: Zhetao Zhang, Wenkun Yu and Giuseppe Casula

Received: 16 August 2022

Accepted: 16 September 2022

Published: 21 September 2022

Publisher's Note: MDPI stays neutral with regard to jurisdictional claims in published maps and institutional affiliations.



Copyright: © 2022 by the authors. Licensee MDPI, Basel, Switzerland. This article is an open access article distributed under the terms and conditions of the Creative Commons Attribution (CC BY) license (<https://creativecommons.org/licenses/by/4.0/>).

1. Introduction

The global GNSS network solution plays an important role in geodesy, especially geodetic parameter estimation [1], high-precision product generation [2,3], datum maintenance [4], and geodynamics applications [5,6]. As a well-developed method, double differencing (DD) [7] is widely used in well-known GNSS data processing software such as Bernese 5.2 developed by Rolf Dach et al. at the Astronomical Institute of the University of Bern (AIUB), Switzerland [8] and GAIMIT/GLOBK 10.7 developed by T. A. Herring et al. from MIT, Scripps Institution of Oceanography and Harvard University in America [9]. How to improve the accuracy of the GNSS DD network is a topic that has been continuously explored.

In the implementation of the GNSS network solution, in order to reduce the computational load while not affecting the overall positioning accuracy, the independent baseline solution of multiple stations should be used before the entire network adjustment [7]. The principle of independent baseline selection is that only one path exists between any two stations, while all the stations should be connected. For a network with n stations, a total of $n(n + 1)/2$ baselines exist, only $n - 1$ of which are independent. The objective of the independent baseline selection is to optimize the overall accuracy of the baseline solutions

in order to facilitate the subsequent network adjustment. Mathematically, this process can be described by the minimum spanning tree (MST) [10,11] problem.

In the process of MST, the criteria for selecting baselines can be defined according to the user's needs. One of the most easily conceived solutions is to make the total length of $n - 1$ baselines the shortest, which is known as the shortest path (SHORTEST) method [7,8]. This is because the shorter the distance between stations, the greater the number of co-viewing satellites, thus more redundant observations are involved to facilitate the network adjustment. More importantly, the tropospheric and ionospheric delays of neighboring stations are similar. The shorter baselines help to better eliminate these errors. Since the original intention of SHORTEST is to improve positioning accuracy by increasing the number of co-viewing satellites, a more straightforward solution is to use the maximum common satellites as the criterion. This method is known as the maximum observation method (OBS-MAX) [8].

Both methods mentioned above have been investigated; for example, SHORTEST was used in a massive GNSS network of more than 2000 globally distributed stations [12], while OBS-MAX is shown to be beneficial in the tropospheric delay estimation [13]. In the ideal situation, the shorter the baseline, the more common observations there are. Then, SHORTEST and OBS-MAX should be fully equivalent. However, the statistics show that they are not consistent [14], i.e., on various days, the baselines generated by different methods could ultimately lead to different solution precision, which violates the assumption that the two methods are equivalent. This means that the number of observations does not necessarily increase as the baseline becomes shorter. This is due to the fact that the satellites are usually not evenly distributed across the sky, e.g., sparse observations in local areas and sufficient co-viewing satellites for some long baselines. In a word, the search for optimal independent baselines is still an open question to be further investigated.

A scheme of setting up weights (WEIGHT) between SHORTEST and OBS-MAX has been proposed [14]. The WEIGHT method was demonstrated to be of higher positioning precision than that of SHORTEST and OBS-MAX. However, how to set up weights lacks theoretical support and can only be empirical. For instance, the weights can be determined based on the posterior accuracy of the final baseline solutions using each of the two methods; on an a priori basis, the Bernese software could use a weight of 30% for the SHORTEST in addition to OBS-MAX as an option [8].

To avoid setting up empirical weights or doubling the computational load brought by a posteriori precision-based weighting, a new method called "observation-density" (OBS-DEN) is proposed here. It takes the ratio of baseline length and the number of observations between two stations as the criterion of the MST. The physical interpretation of this criterion is the number of common satellites per unit distance, which overcomes the degradation of baseline accuracy by seeking only maximum observations or the shortest baselines. The advantage of OBS-DEN is that it provides an explainable weighting scheme that can overcome the downsides of SHORTEST and OBS-MAX. This method can be used in various types of GNSS network solution-related software, alongside existing options for users to choose from.

The rest of the paper is organized as follows. In Section 2, the datasets and products, the principle of MST, and the criterion with OBS-DEN are introduced. Then the flowchart for generating independent baselines using various methods and the parallelization of network processing is presented in Section 3. Afterward, the results of single-day solutions and annual statistics are analyzed and discussed in Section 4. Finally, the paper is concluded in Section 5.

2. Data and Method

2.1. Data

Observation data from about 100 IGS stations distributed worldwide, was used to test the proposed method. The data was in Receiver Independent Exchange Format (RINEX) and can be accessed through (<https://cddis.nasa.gov/archive/gnss/data/daily/2012/>,

Weihai, China, 1 June 2018). First, data from 13 January 2012, was used to show the accuracy of a single-day solution. After that, data from the whole year 2012 was used for statistical analysis. We chose a data span over the year 2012, as it was the first peak of the last solar cycle [15], which helps to investigate the performance of the proposed method under various ionospheric situations.

Both GPS and GLONASS observations were included in the processing. The sampling interval of the data was 30 s. Precise products, including the precise orbit and clocks (*.SP3 and *.CLK), Earth rotation parameters (*.ERP), ionospheric parameters (*.ION), differential code biases (*.DCB), reference coordinates (*.CRD), antenna phase center corrections, receiver types, and tidal loading corrections (*.BLQ and *.ATL) were adopted to enable high-precision GNSS network solution. The data was processed with the Bernese software developed at the Astronomical Institute of the University of Bern (AIUB). Detailed descriptions or flow charts of data processing with Bernese can be found in the Bernese manual [8] or other publications [12,14,16–18]. The products were downloaded and used following the website (https://cddis.nasa.gov/Data_and_Derived_Products/GNSS/GNSS_product_holdings.html, Weihai, China, 1 June 2018) and the instruction of Bernese [8].

2.2. MST

MST is the mathematical basis for GNSS DD independent baseline solutions given the baseline length and the number of observations that are calculated and counted. Let V denote all possible Vertexes and E denote all possible edges. Let e denote an edge and $w(e)$ denote the criterion of that edge. This criterion $w(e)$ can be distance or any other weighting factors. MST is defined as follows. In an undirected graph $G = (V, E)$, if there exists a subset T of E , such that the sum of $w(e)$ of e that can connect all nodes (V) is minimal, then that subset T is called the minimum spanning tree of E , or the minimum weight spanning tree.

In geometry, the brief explanation of MST is that it is the shortest path that connects all n nodes. It is easy to understand that there are always $n - 1$ edges in an MST, and these edges are independent, i.e., the path between any of two nodes is unique. The schematic diagram is shown in Figure 1. Usually, the solution of MST can be obtained using the Kruskal method [19,20] or the Prim method [21,22].

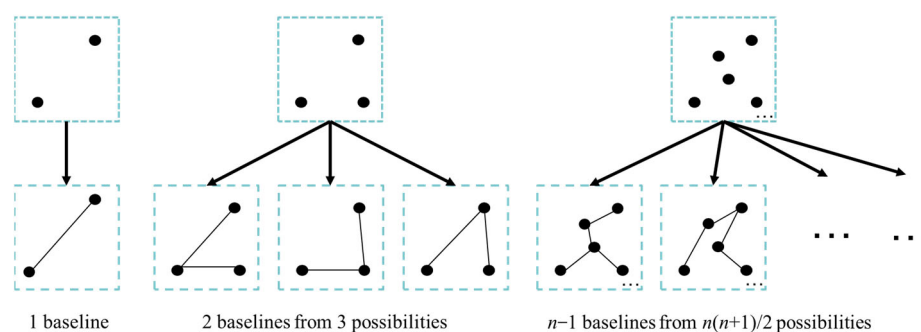


Figure 1. The schematic diagram for selecting the minimum spanning tree from all possibilities.

2.3. The Criteria—Distance, Observation, and Others

The goal of the baseline selection is to optimize the overall accuracy of baseline solutions. For the SHORTEST method, only the length of the path is used as the criterion. Mathematically, the weight $w_{\text{SHORTEST}}(e)$ in MST is proportional to the baseline length, i.e., the smaller the baseline length, the smaller $w_{\text{SHORTEST}}(e)$ is. This is based on the assumption that the closer two stations, the more thoroughly common errors can be eliminated or reduced by DD, thus the higher overall accuracies can be achieved for baseline solutions. For the OBS-MAX method, on the other hand, only the number of DD observations is used as the criterion, i.e., $w_{\text{OBS-MAX}}(e)$ is considered to be inversely proportional to the number of observations. The more the DD observations, the smaller $w_{\text{OBS-MAX}}(e)$ is. This strategy is based on the fact that more observations can bring higher

redundancy in parameter estimation. WEIGHT is a synthesis of these two strategies. In this process, a normalization is introduced since the dimensions of OBS-MAX (number) and SHORTEST (meter) are not consistent [14]. Unfortunately, WEIGHT is still an empirical operation lacking theoretical support.

Since both shorter baselines and more observations can result in higher accuracies for baseline solutions, it is reasonable to adopt a special weight for MST which is both proportional to the length of the path and inversely proportional to the number of observations. The proposed criterion, i.e., the number of DD observations per unit distance, can be interpreted as the density of the observations over baselines. Thus, the proposed method is named observation-density (OBS-DEN).

Equation (1) represents the definition of $w(e)$ in different baseline selection methods.

$$\begin{cases} w_{\text{SHORTEST}}(e) = m_{\text{sho}} \\ w_{\text{OBS-MAX}}(e) = 1/m_{\text{obs}} \\ w_{\text{WEIGHT}}(e) = x_1/norm(m_{\text{obs}}) + x_2 \times norm(m_{\text{sho}}), \quad (x_1 \geq 0, x_2 \geq 0, x_1 + x_2 = 1) \\ w_{\text{OBS-DEN}}(e) = m_{\text{sho}}/m_{\text{obs}} \end{cases} \quad (1)$$

where m_{obs} denotes the number of co-viewing satellites observed by every two stations, m_{sho} denotes the geodetic distance of each two stations; x_1 and x_2 denote the weights applied to the m_{obs} and m_{sho} factors, respectively, which can be obtained empirically or based on the a posteriori accuracies of the solutions of the two methods. Note that in this paper, the number of observations is counted on a daily basis.

2.4. The Calculation Process of the Independent Baseline

The calculation process is illustrated in Figure 2. First, the observation files of all stations are loaded. After that, the co-observations between every two stations are retrieved per epoch. The total co-observations of each station pair of a day are aggregated, respectively. In this way, the common observation matrix \mathbf{M}_{obs} is formed, and each element m_{obs} represents the number of common observations between every station pair. At the same time, the geodetic distance between every station pair is calculated to form the distance matrix \mathbf{M}_{sho} . The unit of element m_{sho} is meter. \mathbf{M}_{obs} and \mathbf{M}_{sho} are shown in Equation (2).

Then, the MST is applied to the matrix \mathbf{M}_{sho} , which chooses the solution that lets the sum of m_{sho} be the smallest. The main diagonal elements of the \mathbf{M} matrix represent all available observations of individual stations or 0 distances, which are not involved in the MST generation.

$$\mathbf{M}_{\text{obs}} = \begin{bmatrix} m_{\text{obs}}^{1,1} & m_{\text{obs}}^{1,2} & m_{\text{obs}}^{1,3} & \cdots & m_{\text{obs}}^{1,n} \\ & m_{\text{obs}}^{2,2} & m_{\text{obs}}^{2,3} & \cdots & m_{\text{obs}}^{2,n} \\ & & \ddots & \ddots & \vdots \\ & & & \ddots & m_{\text{obs}}^{n-1,n} \\ & & & & m_{\text{obs}}^{n,n} \end{bmatrix}, \quad \mathbf{M}_{\text{sho}} = \begin{bmatrix} m_{\text{sho}}^{1,1} & m_{\text{sho}}^{1,2} & m_{\text{sho}}^{1,3} & \cdots & m_{\text{sho}}^{1,n} \\ & m_{\text{sho}}^{2,2} & m_{\text{sho}}^{2,3} & \cdots & m_{\text{sho}}^{2,n} \\ & & \ddots & \ddots & \vdots \\ & & & \ddots & m_{\text{sho}}^{n-1,n} \\ & & & & m_{\text{sho}}^{n,n} \end{bmatrix} \quad (2)$$

For the matrix \mathbf{M}_{obs} , the reciprocal of each element or the maximum spanning tree should be used, since the largest observation needs to be chosen instead of the smallest. Correspondingly, the WEIGHT matrix \mathbf{M}_{wei} and the OBS-DEN matrix \mathbf{M}_{den} can be computed as follows:

$$\begin{cases} \mathbf{M}_{\text{wei}} = x_1 \times \mathbf{M}_{\text{sho}} + x_2/m_{\text{obs}}, \quad (x_1 \geq 0, x_2 \geq 0, x_1 + x_2 = 1) \\ \mathbf{M}_{\text{den}} = \mathbf{M}_{\text{sho}}/m_{\text{obs}} \end{cases} \quad (3)$$

In the subsequent experiment and data analysis, both x_1 and x_2 of the WEIGHT were set to 0.5. In order to apply the above methods with Bernese, the generated baseline file can be used to replace the baseline file generated by Bernese’s default scheme. Except for the independent baseline option, all other processing sessions and parameter settings follow Bernese’s default options [8].

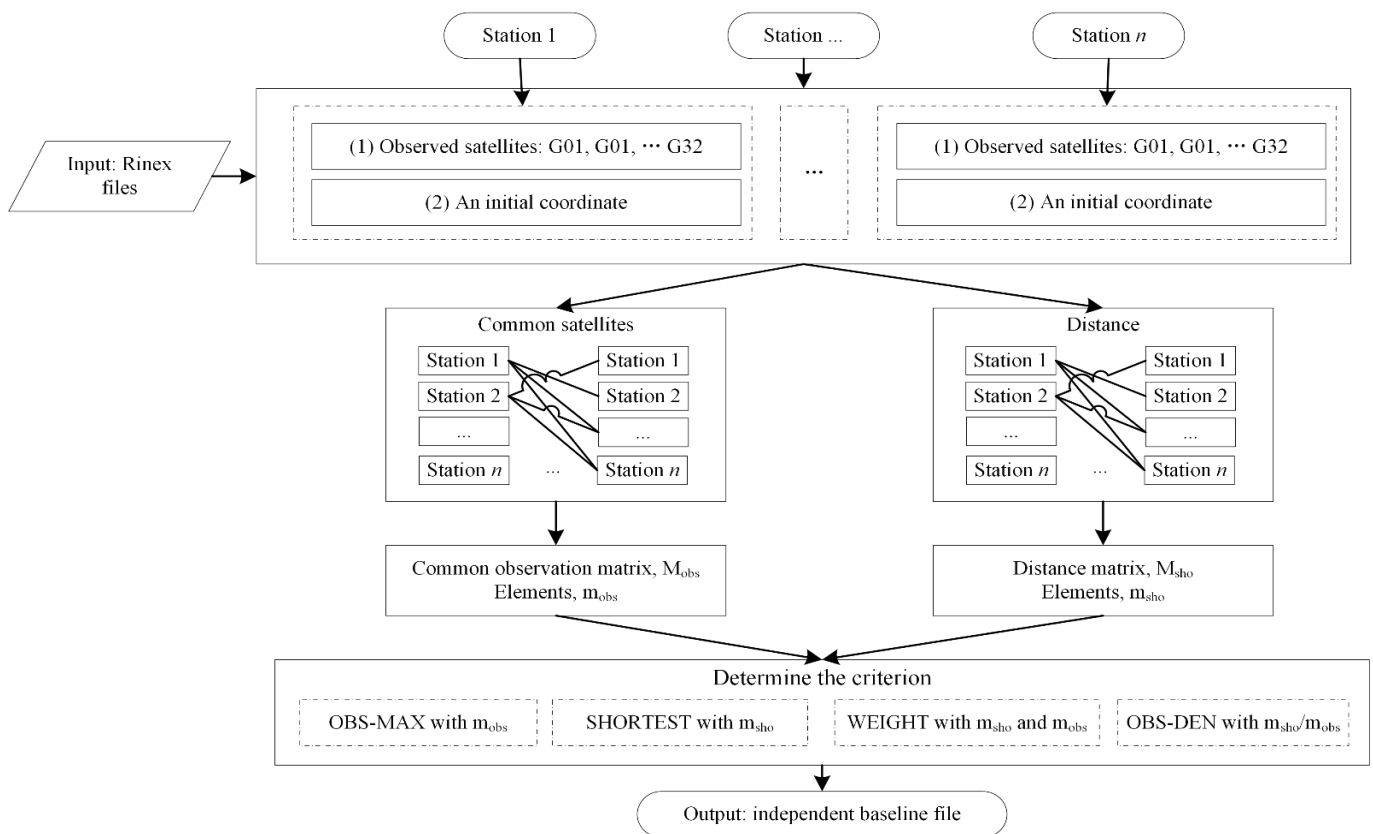


Figure 2. Flow chart for independent baseline selection, starting from reading the RINEX files of all stations, to generate different independent baseline files according to different baseline selection strategies.

2.5. Parallel Computation

Since the data of a global GNSS network may be very large, parallel computation [12,16–18,23] is recommended for such data processing. This can be done by utilizing the Bernese Processing Engine (BPE). As shown in Figure 3, first, the CPU file that comes with Bernese needs to be defined. After that, commands are submitted to the supercomputing platform, the main server of which accepts the commands and performs parallel computation according to the settings in the CPU file. In this experiment, the parallel computation was performed in two different layers, one was the parallelization of the BPEs for a single-day solution of independent baselines, and the other was the parallelization of multiple daily solutions.

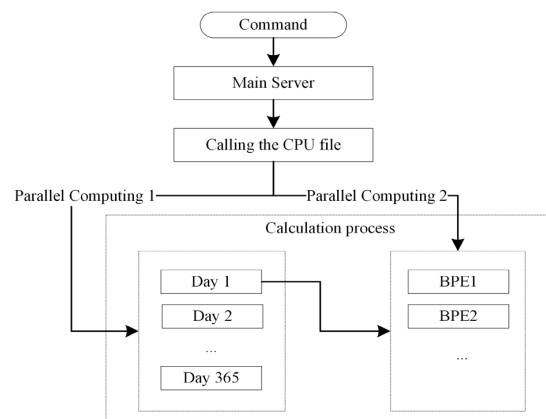


Figure 3. Flowchart of parallel computing.

3. Results

This section first shows the results of a single-day solution, including a comparison of the precision of the different methods, and the generated baseline map for our proposed method. The number of observations versus baseline length is also analyzed. After that, statistical results for one year using different methods are shown.

3.1. Single-Day Solution

At first, an experiment was conducted using globally distributed stations on 13 January 2012. The GNSS network solution was performed in the ITRF08 (International Terrestrial Reference Frame 2008). After the network adjustment, the results were converted to the local ENU (East-North-Up) coordinate system using the final coordinate products in SINEX format (Solution Independent Exchange Format) provided by CODE (Center for Orbit Determination in Europe) as a reference.

As is shown in Table 1, OBS-DEN has the smallest 3D RMS error of 7.30 mm, followed by SHORTEST. For SHORTEST, the large error in the E direction drags down its RMS. Compared with the commonly used OBS-MAX and SHORTEST, OBS-DEN has mainly improved the East and North accuracies.

Table 1. Accuracy comparison of single-day solutions of different methods. The statistics of station accuracies are calculated in the local coordinate system. The three axes of the local coordinate frame are East (E), North (N), and Up (U). The left, middle and right columns show the mean, the standard deviation (STD), and the root mean square (RMS) of the station coordinate errors of each method, respectively.

	MEAN (mm)			STD (mm)			RMS (mm)			
	E	N	U	E	N	U	E	N	U	3D
SHORTEST	−0.99	0.89	−0.53	3.66	3.15	5.97	3.79	3.28	6.00	7.81
OBS-MAX	−0.70	−1.09	0.13	2.83	3.53	7.28	2.92	3.69	7.28	8.67
WEIGHT	−1.45	0.29	0.00	2.96	3.07	6.95	3.30	3.08	6.95	8.29
OBS-DEN	−0.70	0.38	0.19	2.78	2.41	6.25	2.86	2.44	6.25	7.30

STD represents the degree of dispersion of the error for all stations. Although OBS-DEN has the lowest 3D RMS error, it has a larger STD compared to SHORTEST in the U direction. The STD of N and U components of OBS-MAX are the largest, which indicates that some individual stations may have large errors with OBS-MAX. Generally, it can be seen that the positioning errors of OBS-DEN are less discrete compared to other approaches.

Histograms of the single-day solution showing the coordinate error distributions in the E, N, and U directions of different methods are presented in Figure 4. In the East direction, the error distribution of OBS-DEN is closest to 0 and has rare discrete bars (> 10 mm), followed by OBS-MAX; the center of the error distribution of WEIGHT deviates from 0 at about −1.4 mm, and there are agminated bars around −5 mm, which makes its precision worse than OBS-DEN and OBS-MAX in East. In the N direction, the errors of OBS-DEN are more concentrated, while OBS-MAX has the most discrete values. For the U component, the results of the various methods are broadly similar, with the errors of OBS-MAX being slightly dispersed.

Figure 5 shows the baseline map of OBS-DEN. Since OBS-MAX emphasizes more DD observations, a ‘STAR’-like shape, i.e., a central station with plenty of observations connected with multiple nearby stations [24,25], will exist in many regions. For example, some stations in South America, Australia, and Europe shown in [14] could connect more than 5 baselines. SHORTEST, on the other hand, has fewer baselines clustered towards the central stations, i.e., most stations are connected to only two or three baselines. As a result of a combination of the above two methods, some of the central stations of OBS-DEN, such as POVE in South America and ALIC in Australia, are connected to four baselines, while other stations are mostly connected to two or three baselines.

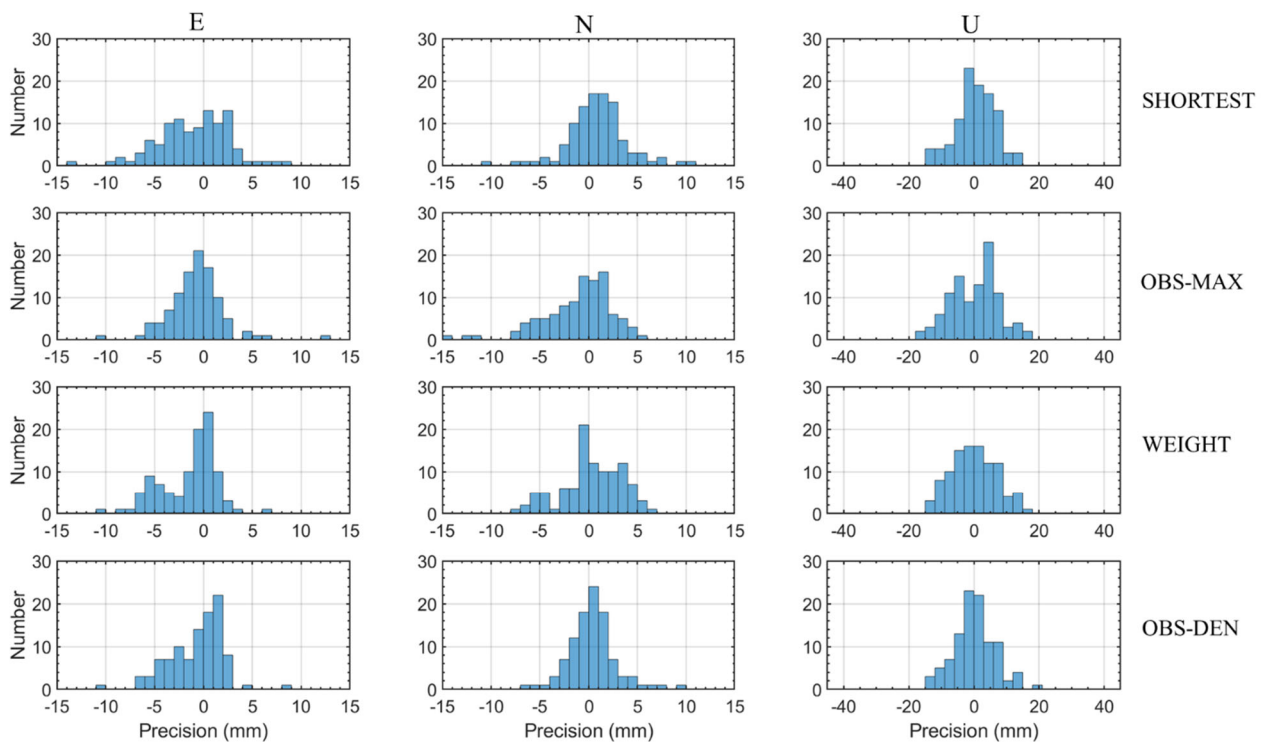


Figure 4. Histograms of single-day solutions. The x-axis of each subplot is the final station coordinate accuracy in millimeters, and the interval of each bin of North and East is 1 mm (3 mm for Up). The y-axis of each subplot represents the number of stations accommodated in each bin. The columns from left to right denote the East (E), North (N), and Up (U) component, respectively. The four methods from top to bottom are SHORTEST, OBS-MAX, WEIGHT, and OBS-DEN, respectively.

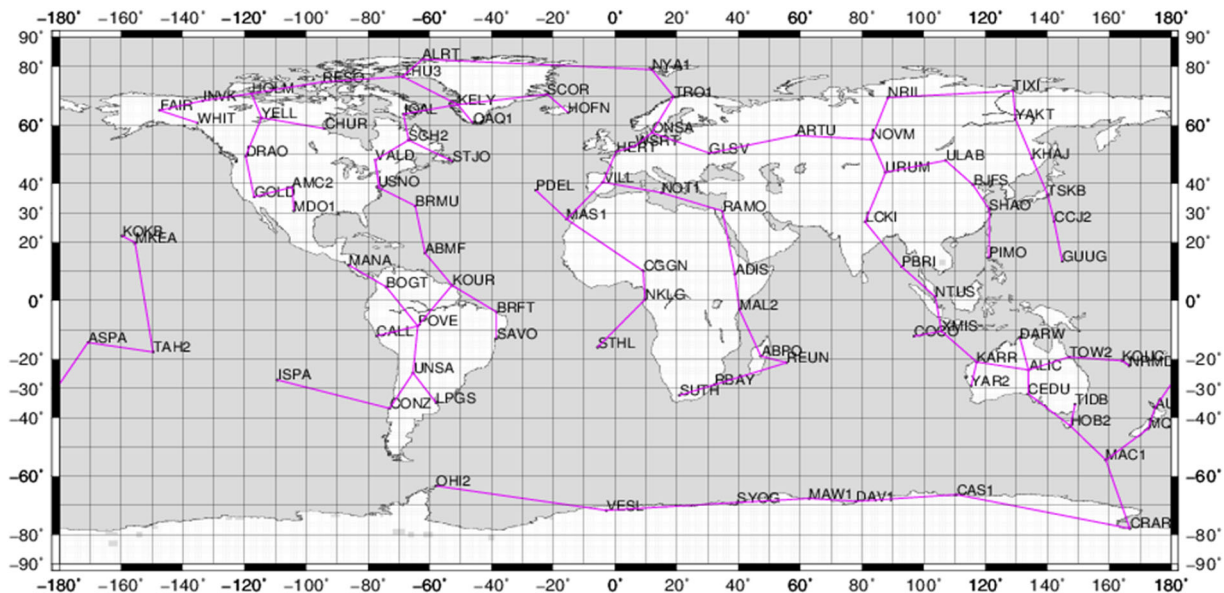


Figure 5. Independent baseline network diagram of about 100 stations generated using OBS-DEN.

The number of DD observations versus the baseline length of each baseline is plotted in Figure 6. It can be seen that the co-viewing satellites decrease roughly linearly with increasing distance. When the station spacing is greater than 17,000 km, the co-viewing satellites are almost absent. However, at distances of several thousand kilometers, there are still large numbers of common observations between stations. It is obvious that the baseline

selection dominated by the number of DD observations, which is applied in OBS-MAX, is no longer applicable at this point. This is due to the long distances resulting in different tropospheric and ionospheric conditions, especially the baselines from mid-latitude to low-latitude/equatorial regions.

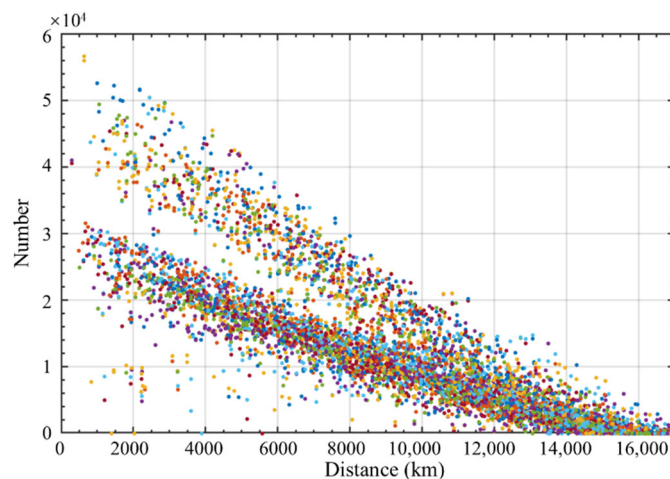


Figure 6. Variation of the number of DD observations between every two stations with distance. This is based on a single-day solution. Some of the stations have only GPS observations while others have both GPS and GLONASS observations, leading to two linear patterns in the plot.

In the data analysis, we found that some stations have both GPS and GLONASS observations while others can receive only GPS signals. That is why there are two linear aggregations presented in Figure 6. In addition to the two obvious linear aggregations, one can see some scattered dots to the lower left. These dots indicate that although the stations are close to each other, there are not many common observations. This may be due to a long-time loss of signal lock or bad observations being excluded. In this case, the baselines are short but with fewer observations. Thus, the SHORTEST method can possibly degrade the accuracy of the baseline solutions due to the introduction of these stations with a small number of observations, while OBS-DEN would avoid such baselines and instead choose baselines with sufficient satellites, but which are slightly longer, i.e., those from the upper-left region of Figure 6.

3.2. One-Year Statistical Results

To better evaluate the performance of various methods, we have tabulated the statistical results for a year. The RMS errors in each direction and the distribution are summarized in Table 2 and Figure 7. Generally, the RMS and the distribution of the methods are comparable. In more detail, the probabilities that 3D errors exceed ε , 2ε , and 3ε mm are presented, respectively, in the right column of Table 2. The threshold ε is set as 9.67 mm, which is the average 3D RMS value of the four methods. From the statistical results, we can see that OBS-DEN has the most stations with accuracies within one ε , and WEIGHT the least. However, the probability that WEIGHT is larger than 2ε and 3ε is the smallest. That is, the coordinate errors of WEIGHT lie more in the interval from ε to 3ε . OBS-DEN and OBS-MAX have more 3D errors larger than 3ε , which pulls down the performance of OBS-DEN and OBS-MAX somewhat.

In addition to the tails of the distributions explored on the right side of Table 2, the histograms showing the coordinate error distributions can be seen in Figure 7. Overall, the distribution of the four methods is similar. However, SHORTEST has fewer burrs for errors greater than 30 mm, especially in the North direction. The distributions of the four methods in the East direction seem to be a little fatter than that in the North, which shows that the STD is minimal in N. For the Up direction, there are large discrete errors around or larger than 50 mm for all four methods.

Table 2. Statistics of one-year solutions. The left side represents the RMS, and the right side represents the probability that the 3D errors for each method exceed certain thresholds. The threshold ϵ is set as 9.67 mm, which is the average 3D RMS value of the four methods.

	RMS				Probability		
	E (mm)	N (mm)	U (mm)	3D	$<\epsilon$	$<2\epsilon$	$<3\epsilon$
SHORTEST	4.38	4.21	7.63	9.75	71.89%	96.17%	99.38%
OBS-MAX	3.92	3.94	7.79	9.57	71.96%	96.54%	99.16%
WEIGHT	4.14	3.92	7.78	9.64	71.82%	96.77%	99.41%
OBS-DEN	4.31	4.15	7.68	9.73	72.49%	96.45%	99.33%

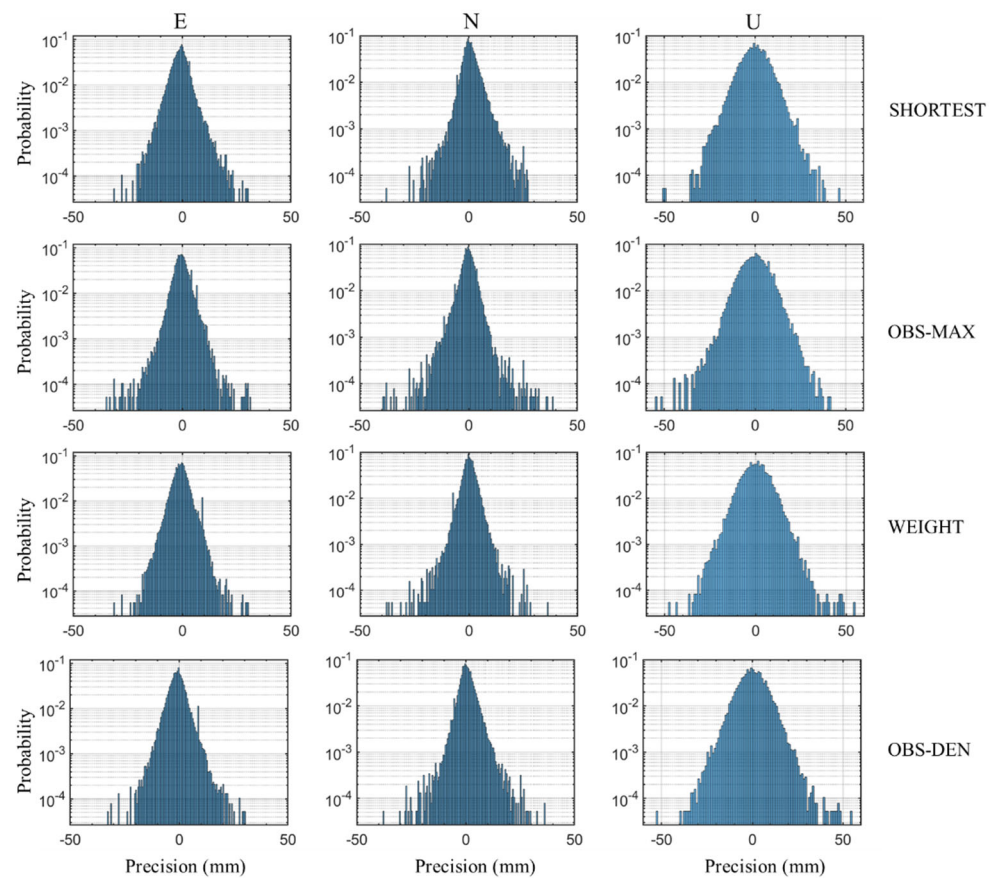


Figure 7. Histograms of one-year solutions. The x-axis of each subplot is the final station coordinate accuracy in millimeters, and the interval of each bin is 1 mm. The y-axis of each subplot, which is on a logarithmic scale, represents the quotient of the number of stations accommodated in each bin and the total number. The columns from left to right denote the East (E), North (N), and Up (U) component, respectively. The four methods from top to bottom are SHORTEST, OBS-MAX, WEIGHT, and OBS-DEN, respectively.

4. Discussion

Overall, OBS-DEN achieves the desired precision in terms of the RMS 3D of station coordinates and shows its capability to get comparable or even better precision than other methods. OBS-MAX is overly focused on the number of observations, but it may include some long baselines with low precision, while SHORTEST is excessively focused on baselines' length and may have incorporated some short baselines with less co-viewed satellites. OBS-DEN excludes these two extreme conditions by both pursuing high observation numbers and also emphasizing short baselines. When compared with WEIGHT, although the accuracy improvement of OBS-DEN is limited, it provides a rational option rather than determining weights empirically.

In theory, with the same information obtained, the final results should be equivalent, but the different ways of data processing led to inconsistent information or data involved. The advantage of OBS-MAX is that it absorbs more redundant observations involved in the adjustment. However, from the above results, especially in Figure 6, there are still a considerable number of observations at a certain range with baselines getting too long. In this case, OBS-MAX may pick some long baselines and make the results worse. In addition to the impacts of the tropospheric and ionospheric delays, the DD ambiguity is more difficult to deal with when the baseline becomes longer [26]. The advantage of SHORTEST is that it uses stations from short baselines whose atmospheric delays are basically the same. However, the shortest baseline could not necessarily exclude the baselines with few co-viewing satellites. As a synthesis of the above two methods, the ratio of the baseline length to the number of observations can be used to overcome the respective shortcomings of the previous individual methods, resulting in a better baseline solution in certain scenarios.

In addition to these most common methods, there are the maximum-ambiguity-fixed-rate method [27] and the STAR method [8]. However, the former uses the outcome of the solution as a basis for selection and cannot provide a pre-defined option for the independent baseline solution as other methods. The STAR method is commonly used for local networks rather than global ones. Therefore, only OBS-MAX and SHORTEST from the traditional methods are involved in the comparison. In future work, the performance of different constellations including positioning accuracy, number of observations, and signal quality could also be used as another baseline searching criteria.

The baseline solution precision is closely related to the station location and density, the shape of the network, and the local atmospheric environment. Different baseline search strategies can be adapted to specific situations. For example, baseline solutions at low latitudes, equatorial and polar regions are usually affected more heavily by ionospheric effects [28,29], especially during a solar maximum period. Thus, more consideration should be given to making the baselines shorter during such periods.

It should be noted that the stations selected for this experiment are globally distributed. The results of these methods may be less different in a local area network where all stations have comparable observations. For example, for a local area network [6] or network RTK (Real-Time Kinetic) [30–32], the different baseline selection methods are theoretically close to being equivalent, especially with a large number of observations of multiple systems [33]. While all stations are close to each other, the number of co-viewing satellites between them is also similar. The baselines selected by different methods may differ from each other, but the total length of the baseline and the total number of satellite observations will not vary significantly.

5. Conclusions

In light of the limitations of current independent baseline selection methods, such as OBS-MAX and SHORTEST, an alternative optimized scheme named OBS-DEN is proposed for GNSS network solutions. It is characterized by maximum co-viewing satellites per unit distance. Since the SHORTEST pursues only short baselines, there is a risk of introducing low-precision baselines with small co-observations numbers; OBS-MAX aims only for more observations and will potentially introduce baselines with large tropospheric and ionospheric differences. OBS-DEN considers both shorter paths and more DD observations in an independent baseline network. It compensates for the shortcomings of SHORTEST and OBS-MAX and does not require empirical weighting. It can be a new independent baseline search strategy for baseline selection in GNSS software, e.g., Bernese.

In both the single-day and annual solutions, OBS-DEN demonstrates its ability to obtain comparable or even higher 3D accuracies. In the single-day solution, the distribution of OBS-DEN is more concentrated. The RMS is smaller than OBS-MAX and SHORTEST. In the statistical results of annual solutions, the 3D RMS of OBS-DEN has the highest probability to be less than 9.67 mm, i.e., the average 3D RMS of all the four methods, compared to other methods.

Due to the uncertainty of the error distribution, OBS-DEN would not be better than other methods in all cases. Different network types and application scenarios correspond to different optimal baseline schemes. In scenarios where the traditional methods are both limited, OBS-DEN can be considered as the preferred scheme.

Author Contributions: Conceptualization, Y.D.; methodology, T.L.; software, T.L. and W.N.; validation, T.L., Y.M., and J.L.; formal analysis, T.L., Y.M., and J.L.; writing—original draft preparation, T.L.; writing—review and editing, Y.D.; visualization, T.L.; funding acquisition, G.X. and W.N. All authors have read and agreed to the published version of the manuscript.

Funding: This research was funded by the Open Fund of the Key Laboratory of Urban Land Resources Monitoring and Simulation, Ministry of Natural Resources, grant number (KF-2021-06-104); Guangdong Basic and Applied Basic Research Foundation, grant number (2021A1515012600); The Opening Project of Guangxi Wireless Broadband Communication and Signal Processing Key Laboratory (No. GXKL06200217); The National Nature Science Foundation of China (No. 42004012); The Natural Science Foundation of Shandong Province (No. ZR2020QD048); Wenhai Program of the S&T Fund of Shandong Province for Pilot National Laboratory for Marine Science and Technology (Qingdao) (NO. 2021WHZZB1004, 2021WHZZB1004_01).

Data Availability Statement: The data and products are downloaded from (www.igs.org, Weihai, China, 1 June 2018).

Acknowledgments: Thanks for the support from the Navigation and Remote Sensing Group of Shandong University. Mowen Li and Zhenlong Fang provided part of the code for data batch downloading; Tianhe Xu, Chunhua Jiang, and Yan Xu provided valuable discussions. This experiment was conducted at the Supercomputing Center of Shandong University in Weihai, China. We also thank Ta-Kang Yeh of Taipei University and Baoqi Sun of the National Time Service Center-Chinese Academy of Sciences, who provided assistance in using and compiling the Bernese software.

Conflicts of Interest: The authors declare no conflict of interest.

References

- Rodriguez-Solano, C.; Hugentobler, U.; Steigenberger, P.; Bloßfeld, M.; Fritsche, M. Reducing the draconitic errors in GNSS geodetic products. *J. Geod.* **2014**, *88*, 559–574. [[CrossRef](#)]
- Stepniak, K.; Bock, O.; Bosser, P.; Wielgosz, P. Outliers and uncertainties in GNSS ZTD estimates from double-difference processing and precise point positioning. *GPS Solut.* **2022**, *26*, 74. [[CrossRef](#)]
- Sun, M.; Liu, L.; Yan, W.; Liu, J.; Liu, T.; Xu, G. Performance analysis of BDS B1C/B2a PPP using different models and MGEX products. *Surv. Rev.* **2022**, *1–12*. [[CrossRef](#)]
- Yang, Y.; Mao, Y.; Sun, B. Basic performance and future developments of BeiDou global navigation satellite system. *Satell. Navig.* **2020**, *1*, 1. [[CrossRef](#)]
- Zajdel, R.; Sośnica, K.; Dach, R.; Bury, G.; Prange, L.; Jäggi, A. Network effects and handling of the geocenter motion in multi-GNSS processing. *J. Geophys. Res. Solid Earth* **2019**, *124*, 5970–5989. [[CrossRef](#)]
- Specht, C.; Specht, M.; Dąbrowski, P. Comparative analysis of active geodetic networks in Poland. *Int. Multidiscip. Sci. GeoConf. SGEM* **2017**, *17*, 163–176.
- Xu, G.; Xu, Y. *GPS: Theory, Algorithms and Applications*; Springer: Berlin, Germany, 2016.
- Dach, R.; Walser, P. *Bernese GNSS Software, Version 5.2*; University of Bern: Bern, Switzerland, 2015.
- Herring, T.; King, R.; McClusky, S. *Introduction to Gamit/Globk*; Massachusetts Institute of Technology: Cambridge, MA, USA, 2010.
- Gilad, E.-T. Graph theory applications to GPS networks. *GPS Solut.* **2001**, *5*, 31–38.
- Graham, R.L.; Hell, P. On the history of the minimum spanning tree problem. *Ann. Hist. Comput.* **1985**, *7*, 43–57. [[CrossRef](#)]
- Cui, Y.; Chen, Z.; Li, L.; Zhang, Q.; Lu, Z. An efficient parallel computing strategy for the processing of large GNSS network datasets. *GPS Solut.* **2021**, *25*, 36. [[CrossRef](#)]
- Stepniak, K.; Bock, O.; Wielgosz, P. Reduction of ZTD outliers through improved GNSS data processing and screening strategies. *Atmos. Meas. Tech.* **2018**, *11*, 1347–1361. [[CrossRef](#)]
- Liu, T.; Xu, T.; Nie, W.; Li, M.; Fang, Z.; Du, Y.; Jiang, Y.; Xu, G. Optimal Independent Baseline Searching for Global GNSS Networks. *J. Surv. Eng.* **2021**, *147*, 5020010. [[CrossRef](#)]
- Krypiak-Gregorczyk, A. Ionosphere response to three extreme events occurring near spring equinox in 2012, 2013 and 2015, observed by regional GNSS-TEC model. *J. Geod.* **2019**, *93*, 931–951. [[CrossRef](#)]
- Chen, Z.; Zhiping, L.; Yang, C.; Hao, L. Parallel computing of GNSS data based on Bernese processing engine. *J. Geod. Geodyn.* **2013**, *33*, 79–82.

17. Li, L.; Lu, Z.; Chen, Z.; Cui, Y.; Sun, D.; Wang, Y.; Kuang, Y.; Wang, F. GNSSer: Objected-oriented and design pattern-based software for GNSS data parallel processing. *J. Spat. Sci.* **2019**, *66*, 27–47. [[CrossRef](#)]
18. Jiang, C.; Xu, T.; Du, Y.; Sun, Z.; Xu, G. A parallel equivalence algorithm based on MPI for GNSS data processing. *J. Spat. Sci.* **2019**, *66*, 513–532. [[CrossRef](#)]
19. Naidoo, K. MiSTree: A Python package for constructing and analysing Minimum Spanning Trees. *arXiv* **2019**, arXiv:1910.08562. [[CrossRef](#)]
20. Kruskal, J.B. On the shortest spanning subtree of a graph and the traveling salesman problem. *Proc. Am. Math. Soc.* **1956**, *7*, 48–50. [[CrossRef](#)]
21. Spira, P.M.; Pan, A. On finding and updating spanning trees and shortest paths. *SIAM J. Comput.* **1975**, *4*, 375–380. [[CrossRef](#)]
22. Prim, R.C. Shortest connection networks and some generalizations. *Bell Syst. Tech. J.* **1957**, *36*, 1389–1401. [[CrossRef](#)]
23. Cui, Y.; Lv, Z.; Li, L.; Chen, Z.; Sun, D.; Kwong, Y. A Fast Parallel Processing Strategy of Double Difference Model for GNSS Huge Networks. *Acta Geod. Cartogr. Sin.* **2017**, *46*, 48–56.
24. Paziewski, J.; Kurpinski, G.; Wielgosz, P.; Stolecki, L.; Sieradzki, R.; Seta, M.; Oszczak, S.; Castillo, M.; Martin-Porqueras, F. Towards Galileo+ GPS seismology: Validation of high-rate GNSS-based system for seismic events characterisation. *Measurement* **2020**, *166*, 108236. [[CrossRef](#)]
25. Fotiou, A.; Pikridas, C.; Rossikopoulos, D.; Chatzinikos, M. The effect of independent and trivial GPS baselines on the adjustment of networks in everyday engineering practice. In Proceedings of the International Symposium on Modern Technologies, Education and Professional Practice in Geodesy and Related Fields, Sofia, Bulgaria, 5–6 November 2009; pp. 201–212.
26. Geng, J.; Mao, S. Massive GNSS network analysis without baselines: Undifferenced ambiguity resolution. *J. Geophys. Res. Solid Earth* **2021**, *126*, e2020JB021558. [[CrossRef](#)]
27. Hua, C. Application Research of Method of Large GNSS Network Realtime Data Rapid Solution. Ph.D. Thesis, Wuhan University, Wuhan, China, 2010.
28. Liu, T.; Yu, Z.; Ding, Z.; Nie, W.; Xu, G. Observation of Ionospheric Gravity Waves Introduced by Thunderstorms in Low Latitudes China by GNSS. *Remote Sens.* **2021**, *13*, 4131. [[CrossRef](#)]
29. Dao, T.; Harima, K.; Carter, B.; Currie, J.; McClusky, S.; Brown, R.; Rubinov, E.; Choy, S. Regional Ionospheric Corrections for High Accuracy GNSS Positioning. *Remote Sens.* **2022**, *14*, 2463. [[CrossRef](#)]
30. Bakula, M.; Przestrzelski, P.; Kazmierczak, R. Reliable technology of centimeter GPS/GLONASS surveying in forest environments. *IEEE Trans. Geosci. Remote Sens.* **2014**, *53*, 1029–1038. [[CrossRef](#)]
31. Wang, P.; Liu, H.; Yang, Z.; Shu, B.; Xu, X.; Nie, G. Evaluation of Network RTK Positioning Performance Based on BDS-3 New Signal System. *Remote Sens.* **2021**, *14*, 2. [[CrossRef](#)]
32. Liu, J.; Zhang, B.; Liu, T.; Xu, G.; Ji, Y.; Sun, M.; Nie, W.; He, Y. An Efficient UD Factorization Implementation of Kalman Filter for RTK Based on Equivalent Principle. *Remote Sens.* **2022**, *14*, 967. [[CrossRef](#)]
33. Siejka, Z. Validation of the accuracy and convergence time of real time kinematic results using a single galileo navigation system. *Sensors* **2018**, *18*, 2412. [[CrossRef](#)]